Effect of cysteine substitutions on the topology of the S4 segment of the *Shaker* potassium channel: implications for molecular models of gating

M.-H. Wang, S. P. Yusaf, D. J. S. Elliott, D. Wray and A. Sivaprasadarao

School of Biomedical Sciences, University of Leeds, Leeds LS2 9JT, UK

(Received 28 July 1999; accepted after revision 28 September 1999)

1. The gating properties of voltage-gated potassium channels are largely determined by the amino acid sequence of their S4 segments. To investigate the nature of S4 movement during gating, we introduced single cysteines into the S4 segment of the *Shaker* potassium channel and expressed the mutants in *Xenopus* oocytes. We then measured the conductance–voltage (g–V) relationships and the rate and the voltage dependence of movement of the engineered cysteines, using p-chloromercuribenzene sulphonate (pCMBS) as a probe.

2. Mutation of charged residues at positions 362, 365 and 368, but not the uncharged residues (positions 360, 361, 363, 364 and 366), to cysteines shifted the g–V relationships to more positive potentials. Mutant channels in which cysteines replaced the charged residues at positions 362 and 365 (R362C and R365C) reacted faster with pCMBS than those in which cysteines were introduced in place of uncharged residues at positions 360 and 361 (I360C and L361C). Furthermore, the R365C mutant channel reacted with pCMBS even at hyperpolarised (−120 mV) potentials. Currents expressed by the doubly mutated R365S/V367C and R368S/V367C channels, but not the singly mutated V367C channel, were inhibited by pCMBS. Moreover, the R368C mutant channel was also affected by pCMBS.

3. Voltage dependence of block by pCMBS (2 min exposure) was steeper for L366C than for L361C and V363C mutant channels (effective charge 2·19, 1·41 and 1·45, respectively). The voltage dependence of the pCMBS effect was also shifted to more depolarising potentials the deeper in the membrane the position of the residue mutated to cysteine (voltages for half-maximal effect −107, −94 and −73 mV for positions 361, 363 and 366, respectively).

4. Our data show firstly that charge-neutralising mutations in S4 alter the topology of this region such that the membrane-spanning portion of S4 is reduced. Secondly, our data for the other mutant channels suggest that S4 might move in at least two sequential steps, and can move up to its maximal limit even at the resting potential of the cell.

Voltage-gated potassium channels comprise a large group of integral membrane proteins, members of which are present in almost all cell types (Hille, 1992; Jan & Jan, 1997). They contain two functional elements, a voltage sensor with which they sense voltage changes across the cell membrane and a selective pore through which K^+ ions permeate (Sigworth, 1994; Jan & Jan, 1997; Yellen, 1998). These functional elements are coupled in such a way that when the membrane is depolarised the sensor detects the change and transmits the signal to the pore which then opens to let potassium ions flow down the electrochemical gradient. Despite numerous studies (Papazian *et al.* 1991, 1995; Seoh *et al.* 1996; Larsson *et al.* 1996; Yusaf *et al.* 1996; Cha & Bezanilla, 1997; Starace *et al.* 1997; Baker *et al.* 1998) the molecular details of this process are still unclear. One reason for this is the lack of three-dimensional structural information for these proteins. Recent X-ray diffraction data (Doyle *et al.* 1998) from crystals of KcsA, a bacterial K^+ channel, have revealed the structure of the pore and have provided an insight into the mechanism by which K^+ channels select K^+ ions over other cations. However, KcsA, unlike voltage-gated K^+ channels, lacks the voltage sensor. For this reason, although the molecular architecture of the pore is now known, the structure of the voltage sensor and the molecular mechanism by which it controls channel opening remain unclear.

In the absence of direct structural data, site-directed mutagenesis, in conjunction with biochemical (Tiwari-Woodruff *et al.* 1997) and electrophysiological (Aggarwal & MacKinnon, 1996; Larsson *et al.* 1996; Yusaf *et al.* 1996; Cha & Bezanilla, 1997; Baker *et al.* 1998) approaches, has been used to investigate the structure of the sensor and the mechanisms by which it controls channel gating. The data suggest that the putative transmembrane segments S2, S3 and S4 together constitute the voltage sensor of the channel.

These segments contain highly conserved charged residues: the S4 segment contains four to seven positively charged residues (arginine or lysine) separated from one another by two hydrophobic residues and the S2 and S3 segments contain negatively charged residues (glutamic or aspartic acid) at conserved positions. Positive charges in S4 are thought to form salt bridges with the negative charges in the S2 and S3 segments and seem to make a major contribution to the gating charge of the channel (Tiwari-Woodruff *et al.* 1997). Some of these charges sense voltage changes across the membrane and move across the transmembrane field. Recent experiments have provided evidence that during depolarisation the S4 segment moves towards the extracellular phase, carrying these gating charges through the transmembrane field (Larsson *et al.* 1996; Yusaf *et al.* 1996; Baker *et al.* 1998).

A large number of voltage-gated K^+ channels have been cloned (Jan & Jan, 1997); they differ from one another with respect to the voltage at which they begin to activate (threshold of activation) and the range of voltage (slope) over which they become fully activated. Changes in these properties can be readily introduced into a channel by mutating residues that contribute to the voltage sensing property of the channel. This has provided the opportunity to examine the relationship between the gating properties and the kinetics of S4 movement using mutants of cloned channels. Accordingly, we have engineered mutations into the S4 segment of the *Shaker* channel, expressed them in *Xenopus* oocytes and, using substituted cysteine accessibility mutagenesis (SCAM) in conjunction with two-electrode voltage clamp, examined the effect of these mutations on S4 movement. Our studies show that: (i) neutralisation of charged residues by replacement with uncharged residues, which shifts the conductance–voltage relationships to the right, alters the transmembrane topology and spatial organisation of the S4 segment, (ii) S4 might move in at least two sequential steps and (iii) S4 movement is highly dynamic, with movements occurring even at the resting potential of the cell. The implications of these new data for the current molecular models of gating are discussed.

METHODS

Molecular biology

All experiments were performed on the *Shaker* B potassium channel Δ(N6–46)ShB1 from which amino acid residues 6–46 have been deleted to remove fast (N-type) inactivation (Hoshi *et al.* 1990). The cDNA encoding Δ(N6–46)ShB1 was subcloned into pKS Bluescript (Stratagene). Site-directed mutagenesis was performed on this construct using the method of Kunkel, as described before (Yusaf *et al.* 1996). cRNA was transcribed for the wild-type and for each of the mutants using T7 RNA polymerase (MEGAscript, Ambion), after linearisation of the plasmid constructs with *Hin*dIII. *p*-Chloromercuribenzene sulphonate (pCMBS, sodium salt, Sigma) and methanethiosulphonate-ethyltrimethylammonium (MTSET, Toronto Research Chemicals) reagents were prepared in frog Ringer solution daily before use.

Electrophysiology

Oocytes were isolated from *Xenopus laevis*, anaesthetised by immersion in 0·2% 3-aminobenzoic acid ethyl ester (Sigma). The animals were then killed by cervical dislocation. Dumont stage V or VI oocytes were selected and injected with 50 nl mutant or wild-type cRNA (15–25 ng) and maintained at 19 °C in modified Barth's solution (88 mM NaCl, 1·0 mM KCl, 2·4 mM $NaHCO_3$, 0·82 mM $MgSO_4$, 0·33 mM $Ca(NO_3)_2$, 0·41 mM $CaCl_2$, 7·5 mM Tris-HCl, pH 7·6, supplemented with 10 000 units l^{-1} penicillin, 100 mg l^{-1} streptomycin). After 1–2 days, membrane currents were recorded at room temperature (22–25 °C) using the two-electrode voltage clamp configuration (Geneclamp 500, Axon Instruments), as previously described (Yusaf *et al.* 1996). Electrodes were filled with 3 M KCl and resistances were 1–3 MΩ and 1–1·5 MΩ for the voltage and current electrodes, respectively. Oocytes were held in a 50 μl chamber and were continually superfused (2 ml min^{-1}) with frog Ringer solution (115 mM NaCl, 2 mM KCl, 1·8 mM $CaCl_2$, 10 mM Hepes, pH 7·2). To measure currents, oocytes were held at −80 mV and 200 ms test depolarisations were applied in 10 mV increments (0·1 Hz) in order to construct current–voltage (*I–V*) relationships. A series of 20 hyperpolarising steps of 10 mV were also applied to allow leak subtraction. Data were filtered at 2 kHz using Geneclamp and then sampled at 4 kHz using CED software and a CED 1401 interface. Leak and capacitance artefacts were removed by subtracting averaged leak subtraction traces from the current traces.

For ease of presentation, mutant channels will be referred to throughout the text as mutants.

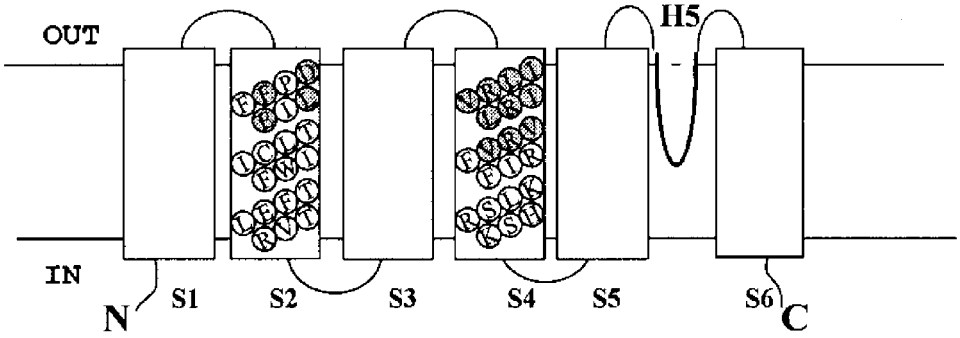

Figure 1. Proposed transmembrane topology of a *Shaker* potassium channel subunit

The putative transmembrane segments (S1–S6) and the pore-forming H5 region are labelled. Proposed sequences of the S2 (residues D279–R297) and S4 (residues I360–K380) segments are shown in the single letter amino acid code. Residues mutated to cysteines are shaded in grey.

RESULTS

Replacement of charged residues in the S2 and S4 segments with cysteines shifts the conductance–voltage relationship to the right

Previous studies (Papazian *et al.* 1991; Aggarwal & MacKinnon, 1996; Seoh *et al.* 1996) have shown that in the *Shaker* potassium channel, replacement of charged residues of the S4 and S2 segments with neutral glutamine or aspargine residues leads to a shift in the voltage dependence of channel activation. In an attempt to explain these shifts in terms of structural changes associated with the activation process, we replaced arginines at positions 362, 365 and 368 and glutamate at position 283 of the *Shaker* channel with cysteines (Fig. 1). Cysteine was substituted rather than glutamine or aspargine because cysteine residues allow the structural changes to be monitored using cysteine modification reagents (Holmgren *et al.* 1996; Larsson *et al.* 1996; Yang *et al.* 1996; Yusaf *et al.* 1996; Baker *et al.* 1998). All four mutants in which cysteine replaced charged residues showed rightward shifts in the conductance–voltage (g–V) relationship when compared with that of the wild-type channel (Fig. 2). SCAM (Holmgren *et al.* 1996; Larsson *et al.* 1996; Yang *et al.* 1996; Yusaf *et al.* 1996; Baker *et al.* 1998) was used to monitor the movement of the engineered cysteines between the membrane bilayer and the extracellular phase.

pCMBS is a suitable probe to monitor the movement of cysteines between the membrane bilayer and the extracellular phase

A variety of cysteine modification reagents are used for SCAM. Among these, the most widely used are the methanethiosulphonate (MTS)-reagents, particularly MTSET (Holmgren *et al.* 1996; Larsson *et al.* 1996; Yang *et al.* 1996; Baker *et al.* 1998; see Fig. 3*B* for structure). We tested the suitability of this reagent by investigating the effect of extracellular application of MTSET on oocytes expressing the *Shaker* R365C and L366C mutants. In agreement with the previous report (Larsson *et al.* 1996), MTSET caused a leftward shift in the I–V relationship of the R365C mutant, at least for voltages below +30 mV (Fig. 3). However, subsequent application of 100 μM pCMBS to the same oocytes produced further inhibition of current expressed by the R365C mutant, suggesting that modification of the channel by MTSET was incomplete and that the I–V curve obtained after the MTSET treatment represented some combination of the properties of the modified and unmodified channels. In contrast, MTSET only marginally inhibited the current expressed through L366C mutants (Fig. 3), but a subsequent application of pCMBS to the same oocytes completely inhibited the currents. This suggests that MTSET failed to access the cysteine at position 366.

Cysteines replacing the S4 arginines at positions 362 and 365 are highly accessible to pCMBS

Figure 4*A* shows the effect of extracellular application of pCMBS on K^+ currents expressed by oocytes injected with mutant cRNA in which the S4 arginines and the S2 glutamate were replaced with cysteines. The currents were elicited by repeatedly pulsing the cell to +40 mV from a holding potential of −80 mV (200 ms duration, 0·1 Hz). pCMBS completely inhibited the currents expressed by the R362C and R365C mutants. However, current expressed by the E283C mutant was only partially (< 20 %) inhibited. In Fig. 4*A*, we have also shown the accessibility of cysteine in

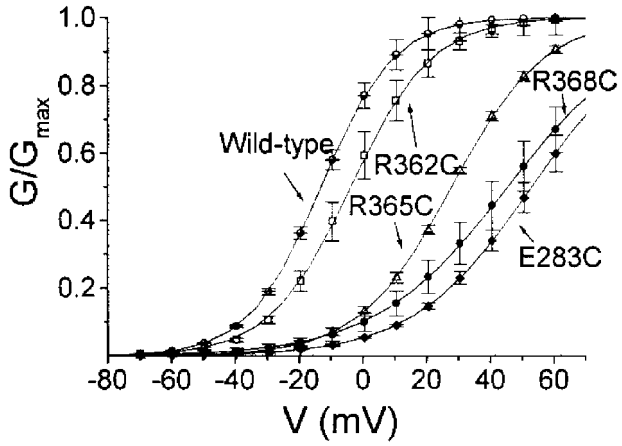

Figure 2. Normalised conductance–voltage (g–V) relationships for mutants in which charged residues were replaced by cysteine

Conductance curves were calculated from macroscopic currents elicited in response to voltage steps (V_{test}) generated using two-electrode voltage clamp. Intracellular K^+ concentration was assumed to be 100 mM. Each data set was fitted by a Boltzmann equation: $G/G_{max} = 1/(1 + \exp(V_{0.5} - V_{test})/k)$, where $V_{0.5}$ is the mid-point of half-maximal conductance and k is the slope factor ($= RT/zF$, where R is the gas constant, T absolute temperature, z the effective charge moved across the width of the membrane and F Faraday's constant). Mean ($n = 5$ or 6) values of $V_{0.5}$ and k, respectively, are as follows: wild-type, −13·2 and 11·3 mV; R362C, −4·3 and 12·5 mV; R365C, 27·8 and 14·3 mV; R368C, 42·8 and 19·8 mV; E283C, 51·2 and 18·0 mV.

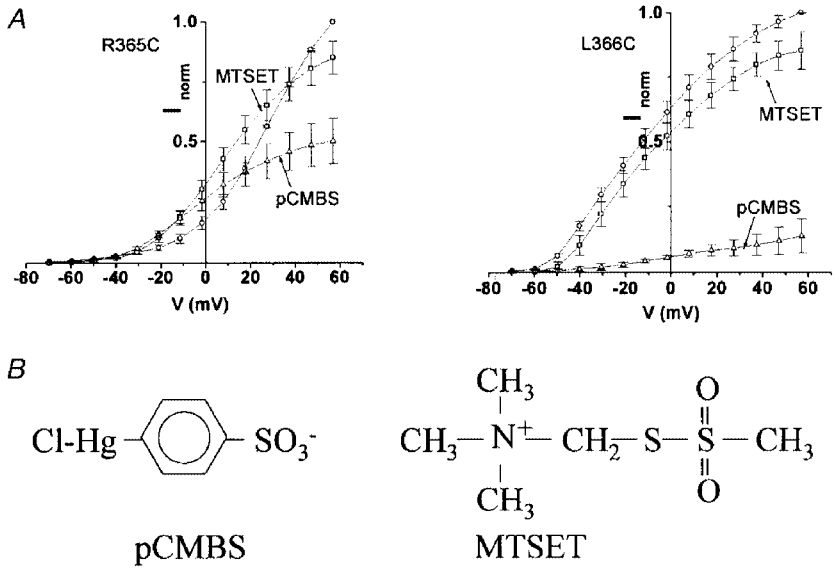

Figure 3. Effects of successive application of MTSET and pCMBS on R365C and L366C mutants

A, *I–V* curves for mutants were first measured in Ringer solution (○). Following this, oocytes were superfused with 5 mM MTSET until the effect reached a steady state and the *I–V* curves (□) were recorded. The oocytes were washed with Ringer solution and then superfused with 100 μM pCMBS until the inhibition reached a steady level before recording the *I–V* curves (△). *B*, molecular structures of pCMBS and MTSET.

the I360C mutant to pCMBS and used this as a reference against which other mutants were compared. The rationale for this is that position 360 is predicted to be at the outer membrane–aqueous interface (Durell *et al.* 1998) and, hence, cysteine placed at this position would be expected to be more accessible to pCMBS than any cysteines engineered downstream of it. However, we found that currents expressed by both R362C and R365C mutants were inhibited as rapidly as that by the I360C mutant, suggesting that R362 and R365 may be closer to the extracellular phase than expected. To study this further, we applied pCMBS to R365C mutants at −80 mV and −120 mV for 2 min in the absence of pulsing. Figure 4*B* shows that over 80% and 50% of the channel activity was inhibited at −80 mV and

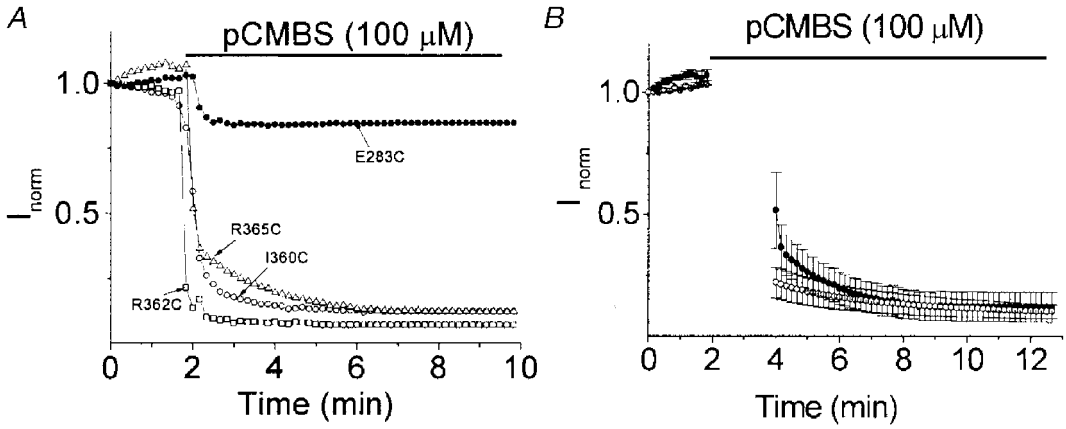

Figure 4. Effect of pCMBS on mutants in which charged residues were replaced by cysteine

A, currents expressed by mutants in which cysteine replaces charged residues are rapidly inhibited by extracellularly applied pCMBS. K^+ currents were recorded from oocytes expressing mutant *Shaker* K^+ channels by repeated pulsing to +40 mV for 500 ms from a holding potential of −80 mV. Ringer solution containing 100 μM pCMBS was applied over the time period indicated by the horizontal bar. Mean normalised current (I_{norm}) values for 5 or 6 oocytes are shown. Data for I360C mutants, showing the effect of pCMBS on cysteine replacing the uncharged residue at the outer membrane border, is shown for comparison. *B*, cysteine in the R365C mutant reacts with pCMBS even at hyperpolarised potentials. Oocytes expressing R365C mutants were depolarised every 10 s by stepping to +40 mV for 500 ms from a holding potential of −80 mV and the currents were recorded. After 2 min, the oocytes were held at −80 (○) or −120 mV (●) in the absence of pulsing and 100 μM pCMBS was applied (as indicated by the horizontal bar). Pulsing was resumed after holding the oocytes at these potentials for 2 min and recordings continued. Data represent means ± S.E.M. ($n = 5$ or 6).

−120 mV, respectively. This suggests that in the resting state of the channel, cysteine in the R365C mutant tends to occupy an extracellularly available position.

As mentioned above, current expressed by the E283C mutant was only partially inhibited by pCMBS. This effect also appears to be due to the removal of charge from the transmembrane position since cysteine mutations of the neighbouring residues, L281C and F279C, and of a residue at the extracellular border of the S2 segment, D277C (which was not implicated in interaction with S4 charges), were unaffected by pCMBS (data not shown). The lack of effect of pCMBS on S2 cysteines suggests that this segment, unlike S4, does not move out of the bilayer.

Effect of pCMBS on R368C mutants

We next investigated the accessibility of cysteine substituted for arginine at 368. The effects of pCMBS on the R368C mutant were found to be highly variable (Fig. 5), from oocyte to oocyte and from batch to batch. While in some oocytes, pCMBS inhibited current expressed by the mutant channels, in others it showed an unexpected activating effect. In several others, pCMBS showed no effect. Because of these inconsistencies, instead of presenting the means of normalised currents, we have shown individual recordings for each oocyte. We have not investigated the reasons for this variation in response. Nevertheless, the data confirm that the cysteine replacing the arginine at position 368 is accessible to extracellular solvent. Whether the cysteine at position 368 is also accessible at negative potentials could not be tested due to the inconsistency of the effects.

Cysteine introduced at position 367 is inaccessible to pCMBS, but becomes accessible when arginines at positions 365 or 368 are neutralised

The above data show that rates of current inhibition for cysteine mutants of charged residues are faster than can be accounted for by the putative position of the residue within the membrane. One possible explanation for this is that charge removal might have altered the topology of S4. To test this further, we neutralised the arginines at positions 365 and 368 by replacing them with serines, which are homologues of cysteine with no known reactivity to pCMBS, and we also introduced a cysteine at position 367. We then tested the sensitivity of these mutants to pCMBS attack. The rationale for this experiment is that pCMBS would attack the cysteine at position 367 only if charge neutralisation affects the topology of S4 (we already know that position 367 is inaccessible to extracellularly applied reagents). Figure 6*A* shows that pCMBS inhibited currents expressed by the doubly mutated R365S/V367C and R368S/V367C channels by about 70 % and 50 %, respectively, while the singly mutated V367C channel was unaffected. *I–V* curves recorded before and after treatment with pCMBS (Fig. 6*B*) indicate that pCMBS reduced the channel current without otherwise altering voltage dependence. These experiments indicate that charge removal from positions 365 or 368 alters the topology of S4 such that in these mutants position 367 becomes exposed to the extracellular phase during depolarisation.

Voltage shifts caused by the neutralisation of R365 and R368 can be reversed by mutating V367 to cysteine

In the above experiments, we observed that, unlike the *I–V* curves of R365C and R368C mutants, which showed rightward shifts, the *I–V* curves of the double mutants were similar to that of the wild-type *Shaker* K^+ channel. To investigate this further, we studied the properties of channels with the single mutations, R365S, R368S and V367C and compared them with those of the channels with double mutations. The *g–V* relationships (Fig. 6*C*) of the charge neutralising serine mutants were similar to those of the corresponding cysteine mutants (Fig. 2) in that they both showed rightward shifts (mean $V_{0.5}$, +19 mV for R365S and +59 mV for R368S), when compared with the wild-type channel. The V367C mutant also showed substantial rightward shift (mean $V_{0.5}$ +29 mV) in its *g–V* relationship. Significant increases in slope values were also observed for all three mutants (see legend to Fig. 6*C*). However, surprisingly, mutants containing changes at both these positions, i.e. the R365S/V367C and R368S/V367C, mutants, showed properties ($V_{0.5}$ and slopes of activation curves) comparable to those of the wild-type channel (Fig. 6*C*). Thus instead of causing a cumulative effect and, thereby, enhancing the positive shifts, the two mutations seem to compensate each other's effects, and restore the near wild-type properties.

Effect of pCMBS on cysteine mutants of neutral S4 residues

Figure 7*A* shows the effect of pCMBS on cysteine mutants of neutral residues (I360, L361, V363, I364, L366, V367 and V369). pCMBS inhibited currents expressed by I360C,

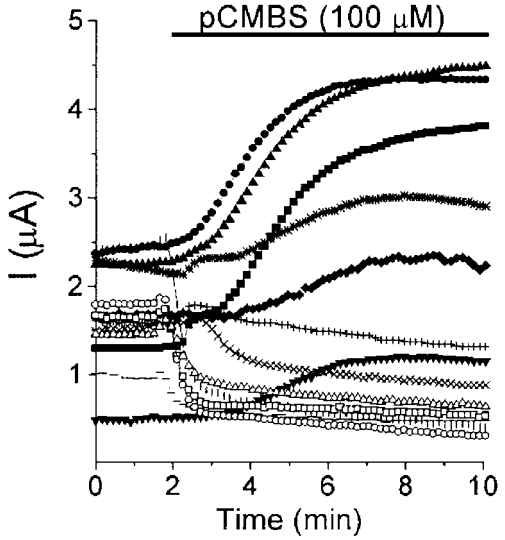

Figure 5

Effects of pCMBS on currents expressed by R368C mutants were recorded from oocytes as described in the legend to Fig. 4. Recordings are shown for individual oocytes.

L361C, V363C, I364C and L366C mutants, but showed no effect on those expressed by V367C and V369C mutants. The current inhibition curves for all pCMBS-sensitive mutants, except I364C, could be described by a single exponential time course. With the exception of I364C, which exhibited bi-exponential inhibition, with a fast and a slow component, the rates of inhibition of pCMBS-affected mutants generally decreased with the increase in the depth of the engineered cysteine within the bilayer. The *I–V* curves of the latter mutants, unlike the channels with mutations of charged residues, were similar to the wild-type *I–V* curve (Fig. 7*B*), suggesting that these mutants have normal S4 topology and the observed differences in the rates, therefore, are due to changes in the accessibility of mutated positions during activation.

We next examined the voltage dependence of extracellular accessibility of cysteines in L361C, V363C and L366C mutants. These three mutant channels were chosen because their kinetics of pCMBS inhibition are monoexponential and slow enough to allow monitoring of their rates over a broad

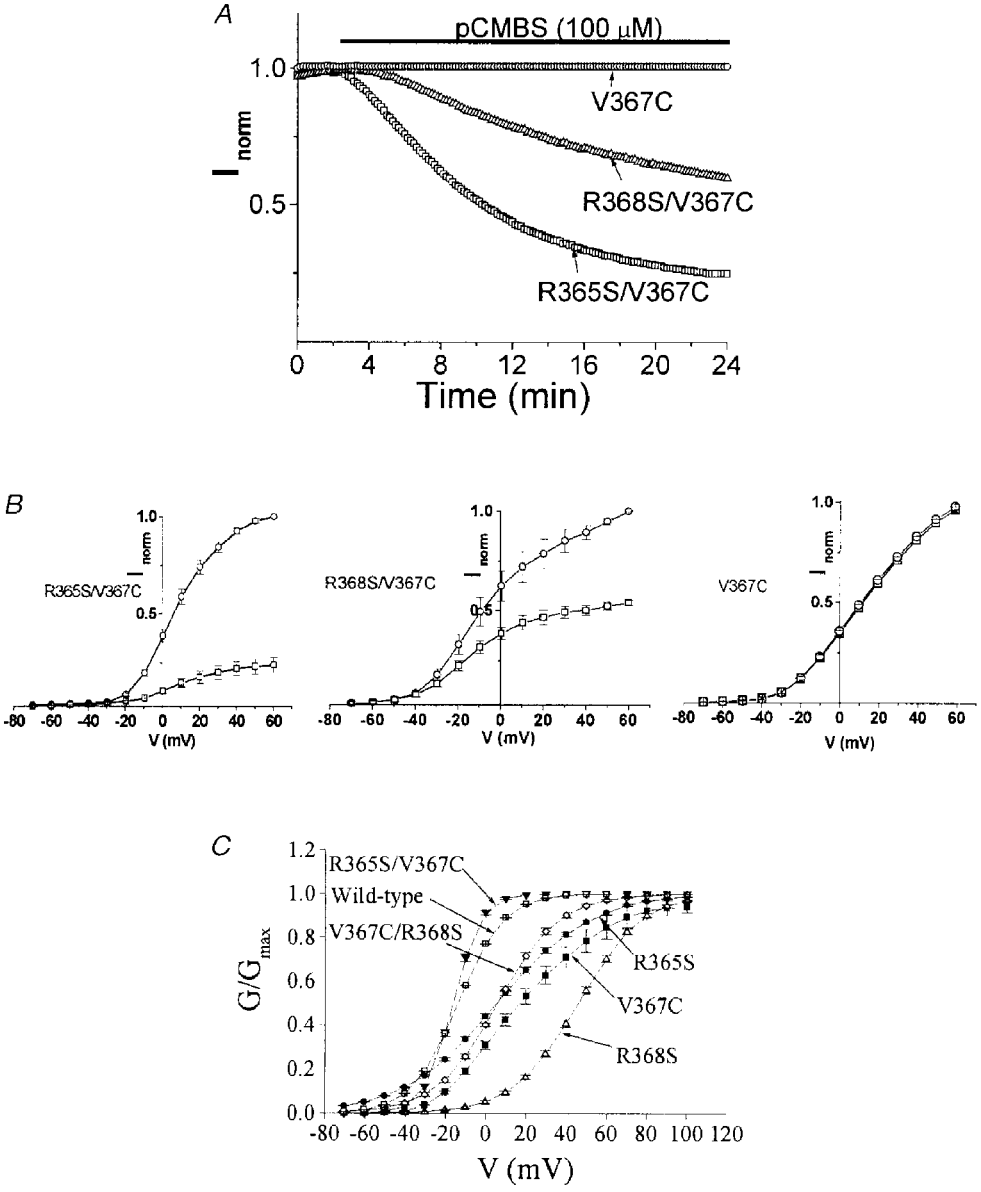

Figure 6. Effect of pCMBS on the doubly mutated R365S/V367C and R368S/V367C channels and the singly mutated V367C channel

A, time course of effect of pCMBS. Currents were recorded as described in the legend to Fig. 4. Each point represents mean normalised current value from 5 or 6 oocytes. *B*, *I–V* curves taken from before (○) and after (□) a 24 min pCMBS (100 μM) application for each mutant. *C*, normalised conductance–voltage relationships for doubly and singly mutated channels were calculated as described in the legend to Fig. 2. Mean values of measured parameters, $V_{0.5}$ and k, respectively, for the wild-type and mutant channels are as follows: wild-type, −13·2 and 11·3 mV; V367C, 15·8 and 20·0 mV; R365S, 5·7 and 23·2 mV; R368S, 46·2 and 16·0 mV; R365S/V367C, −16·2 and 7·3 mV; R368S/V367C, 5·4 and 14·9 mV.

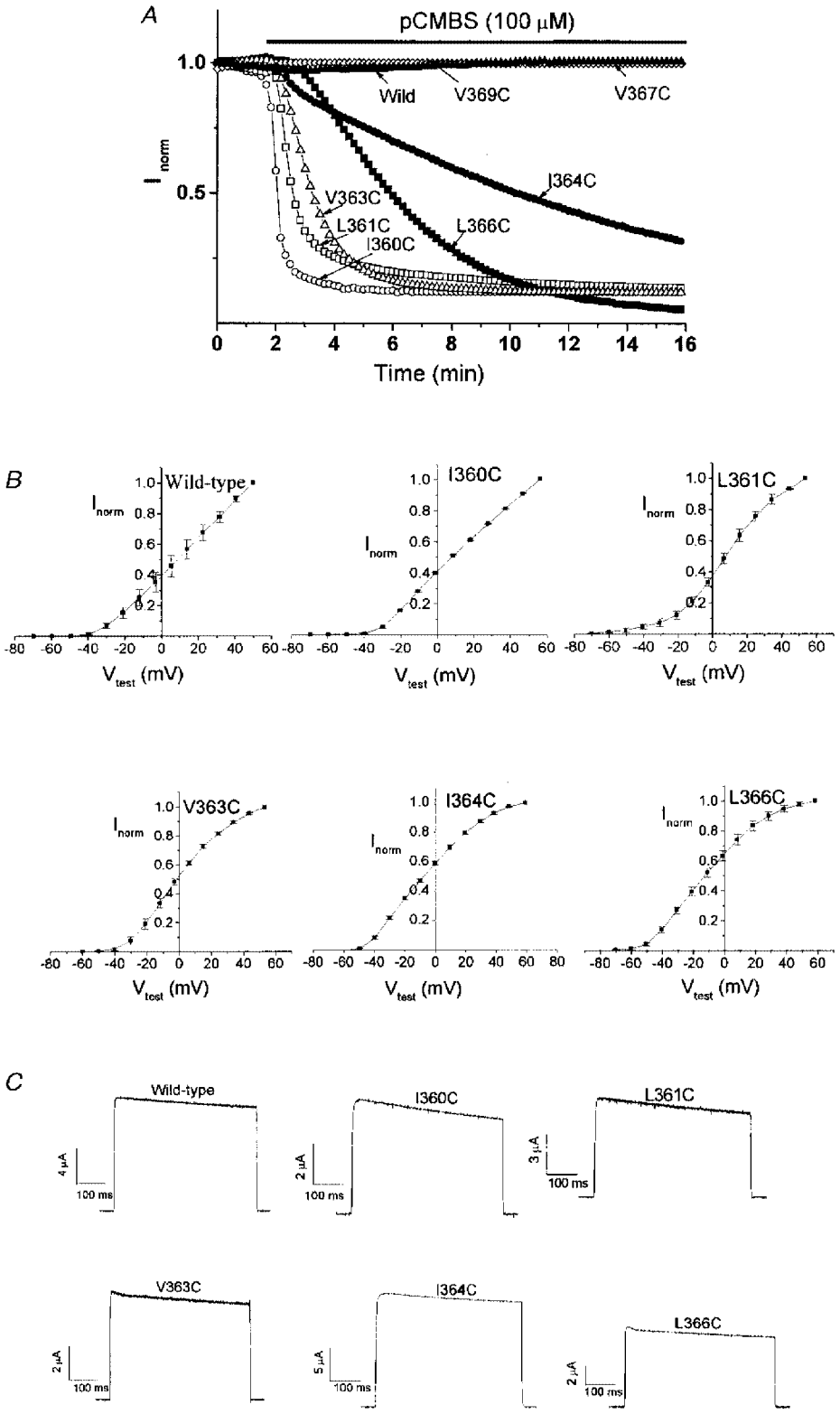

Figure 7. Effect of pCMBS on channels with cysteine mutations of uncharged residues

A, currents were recorded from oocytes expressing the indicated mutants and the effect of pCMBS was studied as described in the legend to Fig. 4. Mean normalised current values for 5 or 6 oocytes are shown. Time constants, estimated from mono-exponential fits, for the various mutants are as follows: I360C, 0·28 ± 0·04 min; L361C, 0·62 ± 0·02 min; V363C, 2·41 ± 0·41 min; L366C, 8·61 ± 0·73 min. The I364C mutant current could best be described by a bi-exponential equation with time constants of 1·07 ± 0·16 and 14·27 ± 0·9 min. *B*, normalised *I–V* curves (each point represents mean ± S.E.M; $n = 5$ or 6) for each mutant was constructed as described in Methods. *C*, time course of mutant currents evoked at +40 mV from a holding potential of −80 mV.

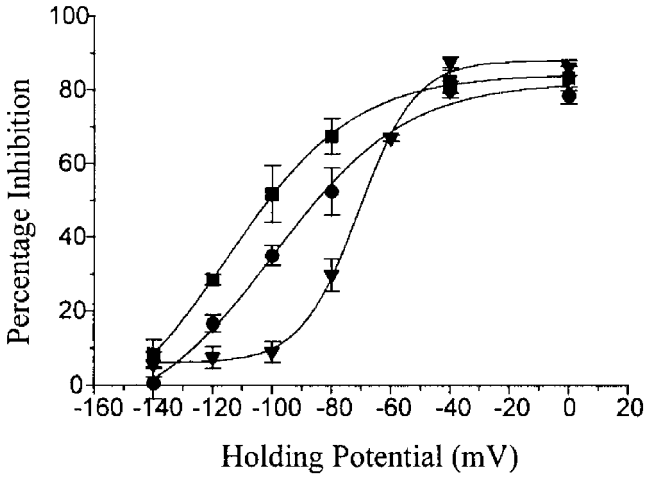

Figure 8. Voltage dependence of pCMBS modification of cysteine mutants

I–V curves were measured (−80 mV holding potential) in Ringer solution from oocytes expressing L361C (■), V363C (●) and L366C (▼) mutant channels. Following this, oocytes were held at the indicated potentials for 2 min and, while still at this potential, superfused with 100 μM pCMBS for 2 min. After washing out the reagent with Ringer solution, *I–V* curves were recorded again from −80 mV holding potential. Percentage inhibition was calculated from the currents at +40 mV before and after pCMBS treatment and is shown plotted against the voltage at which pCMBS was applied. The data were fitted by a least-squares method with the Boltzmann equation: $\Delta I = I_{max}/(1 + \exp(-z(V_m - V_{0.5})/kT))$, where ΔI is the percentage inhibition, I_{max} the maximal percentage inhibition, V_m the holding potential, $V_{0.5}$ the potential for half-maximal inhibition, k the Boltzmann constant, T the absolute temperature and z the effective charge moved across the width of the membrane. The mean values of measured parameters $V_{0.5}$ and z, respectively, are as follows: L361C, −107 mV and 1·41; V363C, −94 mV and 1·45; L366C, −73 mV and 2·19.

voltage range. In these experiments, oocytes expressing the mutants were held at various potentials (−140 to 0 mV) in the absence of test pulses and treated with pCMBS for 2 min. Following this, the oocytes were washed with Ringer solution to remove unreacted pCMBS and the remaining currents were measured. Figure 8 shows a plot of percentage current inhibited by pCMBS as a function of holding potential at which pCMBS was applied. While the slopes of the curves, which reflect the voltage dependence of exposure of the cysteine in a given mutant, were shallow and similar for L361C ($z = 1{\cdot}41$) and V363C ($z = 1{\cdot}45$) mutants, the slope was much steeper for the L366C mutant ($z = 2{\cdot}19$) (see the legend to Fig. 8). The values for half-maximal inhibition ($V_{0.5}$) became more positive with the increase in depth of the engineered cysteine in the membrane, from −107 mV for L361C to −94 mV for V363C

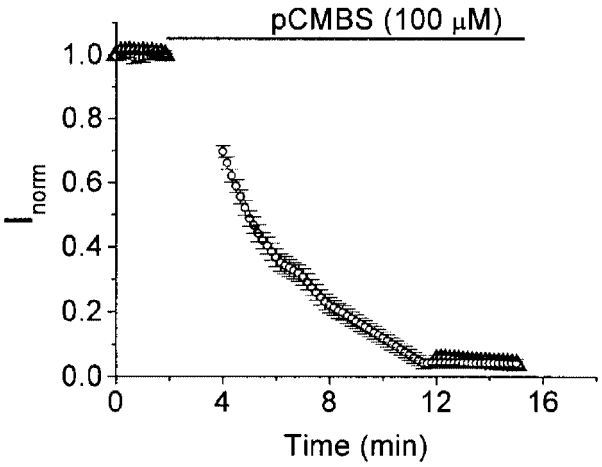

Figure 9. Maximal exposure of S4 can occur even at −80 mV

Oocytes expressing the L366C mutant were depolarised every 10 s by stepping to +40 mV for 500 ms from a holding potential of −80 mV and the currents were recorded. After 2 min, the oocytes were held at −80 mV in the absence of pulsing and 100 μM PCMBS was applied (indicated by the horizontal bar) for 2 (○) or 10 min (●). Following this, pulsing was resumed and the recordings continued. Data represent means ± S.E.M.; $n = 5$ or 6.

to −73 mV for L366C mutants. Since the time courses of inhibition of these three mutants are different, it would be worth examining the voltage dependence of inhibition using longer exposure times, in order to eliminate the possibility that the observed differences in the steepness of the curves are not due to differences in the rates of modification.

Maximal exposure of S4 can occur even at −80 mV

Previous studies (Yusaf *et al.* 1996) have shown that L366 represents the last residue up to which the S4 segment is exposed to the extracellular phase during depolarisation. The data in Fig. 8, however, indicate that this residue can be exposed even in the absence of depolarisation; about 30 % of L366C currents were inhibited during the 2 min exposure to pCMBS at −80 mV. When exposure to pCMBS was prolonged (10 min), complete inhibition of currents occurred (Fig. 9); this confirms that L366 can move outward even at the resting potential of the cell.

DISCUSSION

Recent studies (Larsson *et al.* 1996; Yusaf *et al.* 1996) have established that in response to depolarisation the S4 segment of voltage-gated K^+ channels moves towards the extracellular phase, carrying its voltage-sensing positive charges (gating charges) through the membrane electric field. Consequently, neutralisation of these positive charges produces large changes in the voltage dependence of channel activation (Papazian *et al.* 1991; Aggarwal & MacKinnon 1996; Seoh *et al.* 1996). In this study, we used SCAM to investigate if these changes can be explained in terms of altered transmembrane movement of S4. We found that neutralisation of charged residues distorts the transmembrane topology of S4 such that the membrane-spanning portion of S4 becomes shorter in the charge-depleted mutants. This observation prompted us to re-examine the current molecular models of S4 movement (Larsson *et al.* 1996; Baker *et al.* 1998), which were developed largely on the basis of experimental data derived from mutations of charged residues. By using mutations of uncharged residues in the present study we show that S4 moves in at least two steps and that maximal movement of S4 can occur even in the absence of membrane depolarisation (i.e. at −80 mV).

Comparison of cysteine modification reagents

In order to follow the S4 movement in the mutant channels we employed SCAM, which involves reaction of engineered cysteines with membrane-impermeant cysteine modification reagents, such as MTSET and pCMBS (Holmgren *et al.* 1996; Larsson *et al.* 1996; Yang *et al.* 1996; Yusaf *et al.* 1996; Baker *et al.* 1998). In order to ascertain which of these two reagents was suitable for our investigation, we compared their effects on R365C and L366C mutants. We found that the reaction of MTSET with the R365C mutant changed the voltage dependence of channel activation whereas pCMBS completely inhibited the currents of this mutant. At the concentration (5 mM) tested, however, MTSET partially bound to R365C, as judged by the fact that a subsequent application of pCMBS to the same oocyte inhibited the currents (Fig. 3). This suggested that not all channels had reacted with MTSET because if they had the reaction would have protected the mutant from subsequent pCMBS attack. This also means that at the end of the reaction with MTSET the mutant currents are heterogeneous reflecting a mixture of unmodified and MTSET-modified channels. Clearly, this would make the quantitative interpretation of the MTSET effects difficult.

The differences in the effects of pCMBS and MTSET can be explained in terms of differences in the chemistries of the two reagents. pCMBS converts cysteine to a mercuri-phenyl–sulphonate conjugate, in other words adding the heavy metal ion Hg^{2+}, a phenyl moiety and the highly charged SO_3^{2-} group ($pK_a < 2$). Addition of these moieties to a critical position in the channel structure would be expected to be highly detrimental to its function (Yusaf *et al.* 1996). The effect of MTSET, on the other hand, is mild and variable; in some it causes activation (Larsson *et al.* 1996), in others it produces inhibition (Larsson *et al.* 1996), and for others it modifies inactivation kinetics (Yang *et al.* 1996). This is most probably because MTSET converts cysteine to a conjugate that is similar in size and net charge to arginine, thereby imparting properties that resemble those of the initial arginine residue. Since the effect of MTSET is mild, it is possible that some modifications may even fail to produce detectable effects and thus could escape detection.

With respect to the L366C mutant, MTSET had little effect, while pCMBS fully inhibited the currents (Fig. 3), indicating that MTSET failed to access the cysteine at position 366. This may also be explained in terms of differences in the chemistries of the two reagents. In pCMBS, the cysteine reacting organic mercuric group is located at the end of the molecule and therefore can more readily access the cysteine in L366C than the thiosulphonate group of MTSET, which is in the middle of the molecule (Fig. 3*B*). Thus despite the fact that MTSET is a very useful reagent, some caution needs to be exercised when interpreting the data. In view of these observations, we chose to use pCMBS in this study.

Neutralisation of S4 arginines alters the transmembrane topology of S4

Since removal of charges makes the channel require more positive potentials to open, we anticipated that the S4 segments of charge-depleted mutant channels might move more slowly and may require more positive potentials to move out when compared with the wild-type channel. However, we found the opposite effect: cysteines (neutral amino acids) replacing the arginines at positions 362 and 365 reacted with the extracellularly applied pCMBS more readily than the cysteines placed near the extracellular border (positions 360 and 361) (Figs 4 and 7), despite the fact that both R362C and R365C mutants required more depolarising potentials than I360C and L361C mutants for channel opening. Moreover, cysteine at position 365 reacted

with pCMBS readily even below the resting potential (−80 mV) of the cell (Fig. 4*B*), while cysteine placed before this position at 361 (hence, presumed to be closer to the extracellular phase) was less readily attacked by pCMBS at this potential (Fig. 8). These data taken together suggest that engineered cysteines in R365C and R362C mutants tend to occupy extracellular positions at the resting potential of the cell.

The data can be interpreted in two ways. The S4 helix may be tilted in the membrane such that positions 362 and 365 face the extracellular phase. Alternatively, the S4 helix may be perpendicular to the membrane in the native channel, with R362 and R365 buried in the membrane, but cysteine substitutions might force a distortion in S4 such that these positions are no longer buried in the bilayer at the resting potential of the cell.

We have obtained two lines of evidence in support of the latter possibility. Firstly, position 367, which does not move into the extracellular phase in the wild-type channel, becomes accessible to extracellular solvent if charges are also removed from positions 365 and 368 (Fig. 6). Secondly, position 368 does not move into the extracellular phase in the wild-type channel (since neither of the neighbouring positions, 367 and 369 are exposed), but becomes accessible to solvent (Fig. 5) when the arginine at this position is replaced by the neutral cysteine. Accessibility of cysteine at 368 to extracellularly applied MTSET has also been recently reported by Baker *et al.* (1998), although the authors interpreted this result as 'protein breathing'. In the latter paper, the authors also cited the unpublished work of M. Holmgren & G. Yellen (Harvard Medical School) according to whom cysteine in position 365 is accessible to MTSET from both phases of the membrane. Taken together, the data strongly argue that removal of conserved charges from their transmembrane location alters the topology of the channel, with resultant redistribution of charges. This was not unexpected, since a number of studies (e.g. Seoh *et al.* 1996; Tiwari-Woodruff *et al.* 1997) have shown that the positive charges of S4 form salt bridges with negative charges in S2 and S3 segments, and suggested that these salt bridges may be critical for the stability of charged segments in the hydrophobic bilayer.

These changes in topology would readily explain the anomalous changes in the gating charge movement in charge neutralising mutants. For example, several studies (Aggarwal & MacKinnon, 1996; Seoh *et al.* 1996) have shown that removal of charges from the conserved positions of S4 results in a decrease in the amount of charge translocated across the transmembrane field, but the decrease is far greater than can be accounted for by simple charge removal. Since the *Shaker* K^+ channel has four subunits, removal of a positive charge from each subunit is expected to produce a decrease of 4 times the elementary charge (e), but the reported (Seoh *et al.* 1996) losses were in the region of $7e$ for these mutants. It has also been observed that in the R365C mutant (Baker *et al.* 1998) and other charge neutralising mutants of position 365 (Aggarwal & MacKinnon, 1996; Seoh *et al.* 1996), gating charge moves in two steps, part of which moves below the resting potential of the cell; the reported $V_{0.5}$ for this component of the R365C mutant is −133 mV (Baker *et al.* 1998). At this potential, however, very little gating charge seems to move for the wild-type channel. Thus removal of positive charge seems to eliminate the salt bridges, or other interactions, required to stabilise the S4 structure within the membrane. As a consequence, there seems to be some rearrangement of S4 charges leading to changes in the folding of the channel protein, leaving fewer gating charges to sense the membrane voltage.

Positive shifts in the voltage dependence of channel activation caused by charge neutralisation can be prevented by mutating the uncharged residue at position 367

In the course of the above studies, we observed that single mutations involving replacement of arginines at positions 365 and 368 with serines, or of valine at position 367 with cysteine, lead to pronounced changes in the voltage dependence of channel activation; all these mutations led to large positive shifts and decreased the steepness of activation curves. However, when the arginine to serine mutation was combined with the replacement of valine 367 with cysteine, the resulting double mutants showed properties comparable to those of the wild-type channel (Fig. 6*C*). The restoration of wild-type properties was rather unexpected, because one would expect that the effect of such double mutations would be cumulative and lead to enhanced rightward shifts and larger changes in the slope of activation curves. Although previous studies (Schoppa *et al.* 1992; Sigworth, 1994; Smith-Maxwell *et al.* 1998) have shown that mutation of uncharged residues also alters the voltage dependence of channel activation, this study demonstrates that it is the overall amino acid sequence, rather than individual residues, that may be important in determining the gating properties of a channel.

S4 moves in more than a single step

In the light of our observation that SCAM studies employing cysteine mutations of charged residues could lead to potentially misleading molecular models of gating, we selected mutants containing cysteine substitutions of uncharged residues to elucidate the molecular steps associated with the S4 movement. Using pCMBS, we studied the rates and voltage dependence of exposure of cysteines introduced at various positions along S4. In general, the rates of current inhibition depended on the position of the cysteine mutation: the inhibition decreased progressively with the depth of the engineered cysteine in the bilayer (Fig. 7). The order of inhibition was: I360C > L361C > V363C > L366C. Assuming that these rates of inhibition represent the rates of exposure of various positions to the extracellular phase, it may be suggested that S4 is unlikely to move in one large step, but rather that it might

move either in a continuous mode (diffusional process), or in a series of small discrete steps, or a combination of both (for a review see Bezanilla & Stefani, 1994).

To obtain further information, we examined the voltage dependence of exposure of three residues, representing the first, middle and the last residues to be exposed of the S4 segment (Fig. 8). We found that the slopes for the voltage-dependent exposure of 361 and 363 were shallow and similar ($z = 1{\cdot}41$ and $1{\cdot}45$, respectively) suggesting that these two residues might move in one voltage-dependent transition. The exposure of residue 366, on the other hand, showed a steep rise ($z = 2{\cdot}19$), indicating that its movement might involve a different transition. Thus S4 movement seems to occur in at least two steps, the first involving segment up to position 363 and the second from 364 up to position 366.

The steep rise for L366C suggests that the latter transition might involve co-operative interactions. Current evidence in fact indicates that co-operative interactions (Tytgat & Hess, 1992; Sigworth, 1994; Smith-Maxwell *et al.* 1998) occur during the later stages of channel activation. Since 366 represents the last residue of S4 to move into the extracellular phase, it seems possible that the exposure of this residue is closely associated with the co-operative interactions between the subunits.

The model is also consistent with a biophysical study (Bezanilla *et al.* 1994) which showed that upon depolarisation, gating charge (q) in the *Shaker* K^+ channel moves in two overlapping kinetic steps: the first step, $q1$, is less voltage dependent and carries about one-third of the charge ($2e$, midpoint −63 mV), whereas the second step, $q2$, is relatively more voltage dependent and carries the remaining two-thirds ($5e$, midpoint −44 mV). It is plausible that the two molecular steps mentioned above correspond to the transitions $q1$ and $q2$. Although cysteines at positions 361 and 363 move in one step, the fact that at any given voltage (−120 to 0 mV), 361 is more accessible to extracellular solvent than 363 suggests that there could be a continuous motion of the segment bordered by these two residues. Thus S4 movement might involve a combination of diffusional motion and discrete steps, as suggested previously (Bezanilla & Stefani, 1994).

Evidence in support of two steps has also been recently reported by Baker *et al.* (1998). They exploited the observation that neutralisation of arginine at 365 by replacement with cysteine separates the two overlapping kinetic steps ($q1$ and $q2$) of the wild-type channel into two distinct components with $V_{0{\cdot}5}$ values of −133 and +1 mV. They introduced cysteines at positions 365 and 370 of S4 and examined the accessibility of these residues to MTSET from both phases of the membrane. These studies led to the proposition that $q1$ is associated with the movement of cysteine at 370 from the intracellular phase into the membrane, and $q2$ with the exposure of cysteine at 365 to the extracellular phase.

S4 can be exposed up to its maximal limit even at the resting potential of the cell

Another unexpected finding of the present work is that the S4 segment can be exposed to the extracellular phase up to its maximal limit (i.e. position 366) even at fairly negative (−80 mV) potentials (Fig. 9). This means that S4 is not static in the membrane, but moves even at the resting potential of the cell. However, the failure to detect any macroscopic currents at this voltage may be due to the fact that the frequency of maximal outward movement is low, and the probability of all four S4 segments moving out simultaneously (which seems to be required for channel opening) would be even less.

Implications of our findings for the current molecular models of gating

Our findings that neutralisation of charged residues alters the topology of S4 have implications for the proposed molecular models of gating (Larsson *et al.* 1996; Baker *et al.* 1998) because these models were built on the basis of data obtained using mutants in which charged residues were neutralised by replacement. The authors argued that the length of the membrane-embedded portion of S4 actually increases from five residues in the closed state to about 12 residues when the channel opens. However, in the light of our current data, we believe that the reported (unprecedented) changes in the thickness of the bilayer during channel activation may be a consequence of the charge-neutralising mutation itself, which places most of the N-terminal part of S4 in an extracellularly accessible environment.

Conclusions

In summary, our data showed that removal of charges alters the membrane topology of S4 in the *Shaker* potassium channel such that its N-terminal end becomes extracellularly exposed. As a consequence, the membrane embedded portion of S4, and hence the gating charge associated with it, is reduced. Our data also suggest that maximal movement of S4 can occur even at very negative potentials and that, in agreement with recent reports, S4 moves in at least two molecular steps, the first involving the segment between residues 360 and 363 and the second including the segment from 364 to 366.

Aggarwal, S. K. & MacKinnon, R. (1996). Contribution of the S4 segment to gating charge in the *Shaker* K^+ channel. *Neuron* **16**, 1169–1177.

Baker, O. S., Larsson, H. P., Mannuzzu, L. M. & Isacoff, E. Y. (1998). Three transmembrane conformations and sequence-dependent displacement of the S4 domain in *Shaker* K^+ channel gating. *Neuron* **20**, 1283–1294.

Bezanilla, F., Perozo, E. & Stefani, E. (1994). Gating of *Shaker* K^+ channels: II. The components of gating currents and a model of channel activation. *Biophysical Journal* **66**, 1011–1021.

Bezanilla, F. & Stefani, E. (1994). Voltage-dependent gating of ionic channels. *Annual Review of Biophysics and Biomolecular Structure* **23**, 819–846.

Cha, A. & Bezanilla, F. (1997). Characterizing voltage-dependent conformational changes in the *Shaker* K^+ channel with fluorescence. *Neuron* **19**, 1127–1140.

Doyle, D. A., Cabral, J. M., Pfuetzner, R. A., Kuo, A., Gulbis, J. M., Cohen, S. L., Chait, B. T. & MacKinnon, R. (1998). The structure of the potassium channel: molecular basis of K^+ conduction and selectivity. *Science* **280**, 69–77.

Durell, S. R., Hao, Y. & Guy, H. R. (1998). Structural models of the transmembrane region of voltage-gated and other K^+ channels in open, closed and inactivated conformations. *Journal of Structural Biology* **121**, 263–284.

Hille, B. (1992). *Ionic Channels of Excitable Membranes*. Sinauer Associates, Sunderland, MA, USA.

Holmgren, M., Jurman, M. E. & Yellen, G. (1996). N-type inactivation and the S4-S5 region of the *Shaker* K^+ channel. *Journal of General Physiology* **108**, 195–206.

Hoshi, T., Zagotta, W. N. & Aldrich, R. W. (1990). Biophysical and molecular mechanisms of *Shaker* potassium channel inactivation. *Science* **250**, 533–538.

Jan, L. Y. & Jan, Y. N. (1997). Cloned potassium channels from eukaryotes and prokaryotes. *Annual Review of Neuroscience* **20**, 91–123.

Larsson, H. P., Baker, O. S., Dhillon, D. S. & Isacoff, E. Y. (1996). Transmembrane movement of the *Shaker* K^+ channel S4. *Neuron* **16**, 387–397.

Papazian, D. M., Shao, X. M., Seoh, S. A., Mock, A. F., Huang, Y. & Wainstock, D. H. (1995). Electrostatic interactions of S4 voltage sensor in *Shaker* K^+ channel. *Neuron* **14**, 1293–1301.

Papazian, D. M., Timpe, L. C., Jan, Y. N. & Jan, L. Y. (1991). Alteration of voltage-dependence of *Shaker* potassium channel by mutations in the S4 sequence. *Nature* **349**, 305–310.

Schoppa, N. E., McCormack, K., Tanouye, M. A. & Sigworth, F. J. (1992). The size of gating charge in wild-type and mutant potassium channels. *Science* **255**, 1712–1715.

Seoh, S. A., Sigg, D., Papazian, D. M. & Bezanilla, F. (1996). Voltage-sensing residues in the S2 and S4 segments of the *Shaker* K^+ channel. *Neuron* **16**, 1159–1167.

Sigworth, F. J. (1994). Voltage gating of ion channels. *Quarterly Reviews of Biophysics* **27**, 1–40.

Smith-Maxwell, C. J., Ledwell, J. L. & Aldrich, R. W. (1998). Uncharged S4 residues and cooperativity in voltage-dependent potassium channel activation. *Journal of General Physiology* **111**, 421–439.

Starace, D. M., Stefani, E. & Bezanilla, F. (1997). Voltage-dependent proton transport by the voltage sensor of the *Shaker* K^+ channel. *Neuron* **19**, 1319–1327.

Tiwari-Woodruff, S. K., Schulteis, C. T., Mock, A. F. & Papazian, D. M. (1997). Electrostatic interactions between transmembrane segments mediate folding of *Shaker* K^+ channel subunits. *Biophysical Journal* **72**, 1489–1500.

Tytgat, J. & Hess, P. (1992). Evidence of cooperative interactions in potassium channel gating. *Nature* **359**, 420–423.

Yang, N., George, A. L. J. & Horn, R. (1996). Molecular basis of charge movement in voltage-gated sodium channels. *Neuron* **16**, 113–122.

Yellen, G. (1998). The moving parts of voltage-gated ion channels. *Quarterly Reviews of Biophysics* **31**, 239–295.

Yellen, G., Sodickson, D., Chen, T. Y. & Jurman, M. E. (1994). An engineered cysteine in the external mouth of a K^+ channel allows inactivation to be modulated by metal binding. *Biophysical Journal* **66**, 1068–1075.

Yusaf, S. P., Wray, D. & Sivaprasadarao, A. (1996). Measurement of the movement of the S4 segment during the activation of a voltage-gated potassium channel. *Pflügers Archiv* **433**, 91–97.

Acknowledgements

We thank the Wellcome Trust for financial support.

Corresponding author

A. Sivaprasadarao: School of Biomedical Sciences, University of Leeds, Leeds LS2 9JT, UK.

Email: a.sivaprasadarao@leeds.ac.uk